Disentangling elastic relaxation and ferroelectric domain contributions to in plane X-ray scattering profile: A necessity in strained ferroelectric superlattices

M. Gharbi, C. Davoisne, F. Le Marrec, L. Dupont, N. Lemée

Disentangling elastic relaxation and ferroelectric domain contributions to in plane X-ray scattering profile: a necessity in strained ferroelectric superlattices

M. Gharbi[1], C. Davoisne[2], F. Le Marrec[1], L. Dupont[2,3] and N. Lemée[1*]

[1]Laboratoire de Physique de la Matière Condensée, UR 2081, University of Picardie Jules Verne, 80039 Amiens, France

[2]Laboratoire de Réactivité et de Chimie des Solides, UMR CNRS 7314, University of Picardie Jules Verne, 80000, Amiens, France

[3]Plateforme de Microscopie Électronique, University of Picardie Jules Verne, 80000, Amiens, France.

*Corresponding author: nathalie.lemee@u-picardie.fr

Abstract

Ferroelectric nanodomains give rise to diffuse X-ray scattering peaks in ultrathin films. Here we study a $Pb(Zr_{0.2}Ti_{0.8})O_3/SrTiO_3$ superlattice, using X-ray diffraction and transmission electron microscopy, We show that both elastic relaxation and ferroelectric nanodomain structuration can contribute to distinct satellite peaks in the X-ray scattering pattern. We show that transmission electron microscopy is required to disentangle elastic relaxation and ferroelectric domain contributions to the in plane X-ray scattering profile.

Keywords: Ferroelectrics, superlattice, thin films, domain structure, X-ray scattering

1. Introduction

Ferroelectric nanostructures are expected to contribute to increase storage densities for ferroelectric memories, and to device miniaturization. For fundamental physics, they constitute fascinating objects to understand ferroelectricity at the nanoscale, since low dimensionality gives rise to new phenomena. In particular as a ferroelectric film becomes thinner, the density of the domains and the domain walls increases and this can play a key role in the functional properties as, for example, in the negative capacitance effect which has recently attracted much attention [1]. Considering a uniformly out of plane polarized material, the polarization discontinuity at the film boundaries creates a depolarizing field that counteracts the polarization. When the screening by free charges is not effective, the stability of the polar phase is preserved by forming a 180° stripe domain of alternate up and down polarization that produces characteristic features in the x-ray scattering pattern [2]. Indeed, the phase contrast between the areas of up and down polarization produces a modulation of the structure factor perpendicular to the domain walls, and is at the origin of satellite peaks. This 180° domain structure has thus been evidenced in ferroelectric thin films [2,3] as well as in ferroelectric/paraelectric superlattices (SLs) [4 – 5]. However, such in-plane modulation can also result from periodic structural defects [6 - 7] or ferroelastic domains [8 - 9] created to minimize the elastic energy. Here we illustrate this point through the study of a $Pb(Zr_{0.2}Ti_{0.8})O_3$ / $SrTiO_3$ SL. Transmission electron microscopy (TEM) and x-ray diffraction (XRD) investigations are combined to disentangle the contributions of the elastic relaxation from the ferroelectric domains structure.

2. Experimental details

The $Pb(Zr_{0.2}Ti_{0.8})O_3$ / $SrTiO_3$ SL was grown starting with a PZT layer, on a single crystal TiO_2 terminated (001) $SrTiO_3$ (STO) substrate, by pulsed laser deposition using a KrF excimer laser (λ = 248 nm) and ceramic targets of $SrTiO_3$ (STO) and $Pb_{1.1}(Zr_{0.2}Ti_{0.8})O_3$ (PZT 20/80). This SL, with wavelength 4.5 nm, is composed of 10 bilayers, each consisting of 5 unit cells of PZT and 6 of STO, which we designate as $[PZT_5/STO_6]_{10}$. The PZT 20/80 and STO layers were deposited at 690 °C in 0.1 mbar of O_2, with a laser fluence of 2 $J.cm^{-2}$ and a pulse rate of 2 Hz. Structural analysis was performed on a high resolution D8 Discover Bruker diffractometer (Cu $K\alpha_1$ radiation, 1.5406 Å). Temperature measurements were carried out in air from room temperature up to 600°C, using a high temperature XRD-chamber. All measurements were reproducible after thermal cycling. The lattice parameter was determined by tracking satellites peaks around the (002) reflection. Microstructural characterization was performed using a TECNAI F20-S-Twin operating at 200kV equipped with a Scanning Transmission Electron Microscope (STEM) function, and a High Angle Annular Dark Field (HAADF) camera giving an image contrast based on atomic number. The cross section samples were prepared by a focused ion beam (FIB) technique after depositing a carbon/platinum bilayer to protect the surface from sputtering.

3. Results and discussion

Figure 1 displays the XRD characterizations of a $[PZT_5/STO_6]_{10}$ SL. The satellite peaks detected in the θ-2θ scan (Fig. 1a) and in the reciprocal space map (RSM) along the [00L] direction (Fig. 1b), are indicative of chemical modulation along the growth direction. Due to the in-plane lattice mismatch (-1.2%) between the PZT layers and STO substrate, elastic relaxation by surface roughening, plastic relaxation by dislocations or by the formation of ferroelastic domains can occur. Indeed when both elastic and

depolarization effects compete with each other, it can lead to a polydomain structure consisting of polarized out of plane c- domains and in plane a- domains [9]. Here, however, the reflections are related only to ferroelectric c- domains. In-plane RSM (Fig. 1c) shows almost coherent growth of the SL to the substrate.

Due to the ferroelectric/paraelectric nature of the $[PZT_5/STO_6]_{10}$ SL, a 180° stripe ferroelectric domain structure is expected to minimize the depolarizing field. These nanodomains can give rise to an in-plane satellite peaks detectable in x-ray scattering perpendicular to the domain walls [10]. The diffraction profile along the [H00] direction (Fig.1d) indicates a complex profile including two types of in-plane modulation. At first sight, the two peaks close to the main Bragg peak could be interpreted as the signal of an in-plane modulation due to the 180° stripe nanodomain structure, corresponding to an average period of 34 nm. Nanodomains are expected to originate from the ferroelectric layers which consist of 5 unit cells. A domain period of 5 nm and 9 nm was respectively reported in a PTO_5/STO_5 SL [11] and in a tricolor SL $[PT_9/STO_2/PZT_{10}]_{20}$ [5], showing the dependence of the domain period on the thickness of the ferroelectric layer. The value of 34 nm is therefore well above what could be expected in a 5 unit cell thick PZT layer: the origin of this 34 nm period must arise from another source. In Fig. 3d (also visible in fig. 3c) a second modulation of very low intensity, around h = +/- 0.09, characterizes a period of around 4.5 nm, coherent with a modulation due to the polar stripe nanodomain structure. The peaks are weak but the domain randomness contributes to their smearing out. [10].

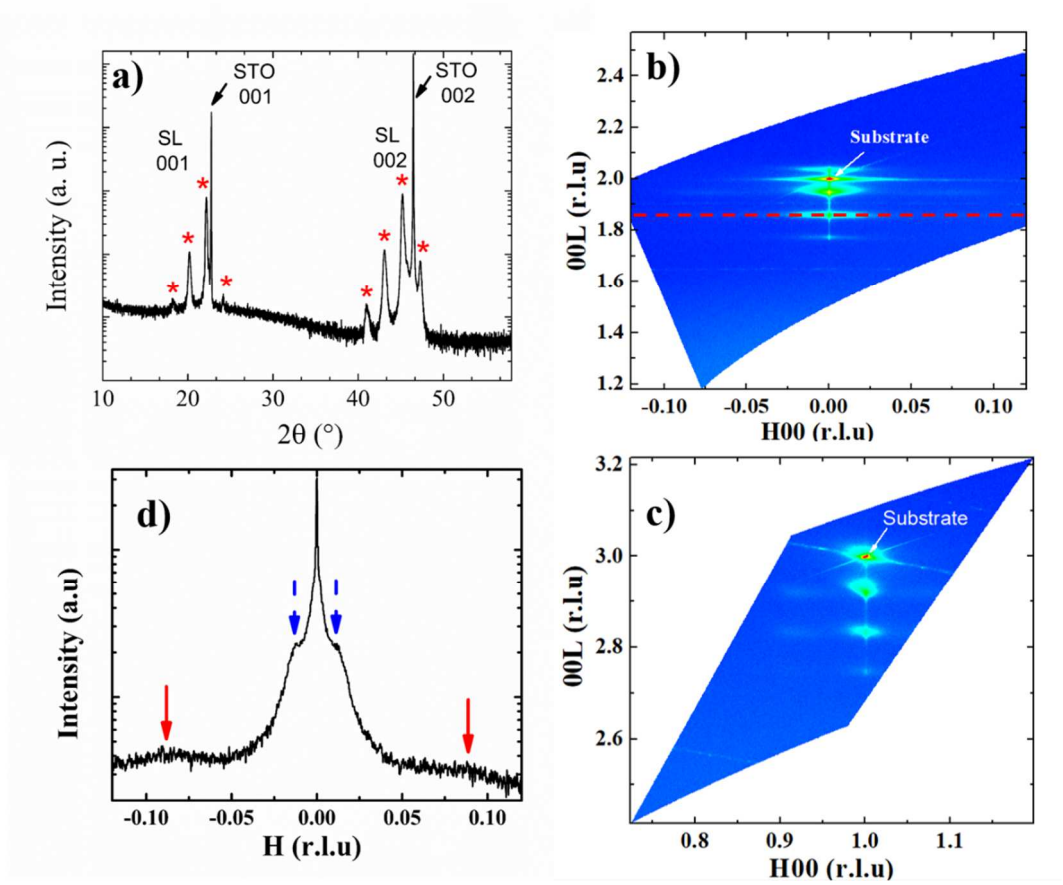

Fig. 1. XRD investigations of a $[PZT_5/STO_6]_{10}$ SL : (a) θ –2θ XRD : the asterisks indicate the satellite peaks, RSM around the (002) (b) and (103) reflection (c), (d) the diffraction profile along the [00H] direction corresponding to the dotted line on the RSM. The plain and dotted arrows indicate, respectively, ferroelectric domains and elastic relaxation. The RSM is plotted in reciprocal-lattice units with respect to the substrate lattice parameter (3.905 Å).

To further explore the 34 nm periodicity, TEM investigations have been carried out on this SL to determine if it could be produced by an ordered arrangement of structural defects. The images displayed in Fig. 2 confirm the absence of a- domains, as no characteristic domain walls between a- and c- phases are evidenced [9]. In Fig. 2b,

the arrangement of alternating white (higher atomic number Z, PZT layers) and grey layers (lower Z, STO layers), confirms the SL periodicity along the growth direction. An almost periodic wave-like modulation with an average period of around 34 nm (+/- 8 nm) is also observed and is coherent with the value estimated from the XRD investigation. This modulation is undoubtedly at the origin of the two satellite peaks close to the Bragg peak in Fig. 1d. Such wave-like modulations have already been reported in SLs characterized by a significant mismatch between the materials involved in the heterostructure [12,13]. Indeed, in these structures, strain is relieved through elastic relaxation by surface roughening. All buried layers grown under stress contribute to the surface roughness.

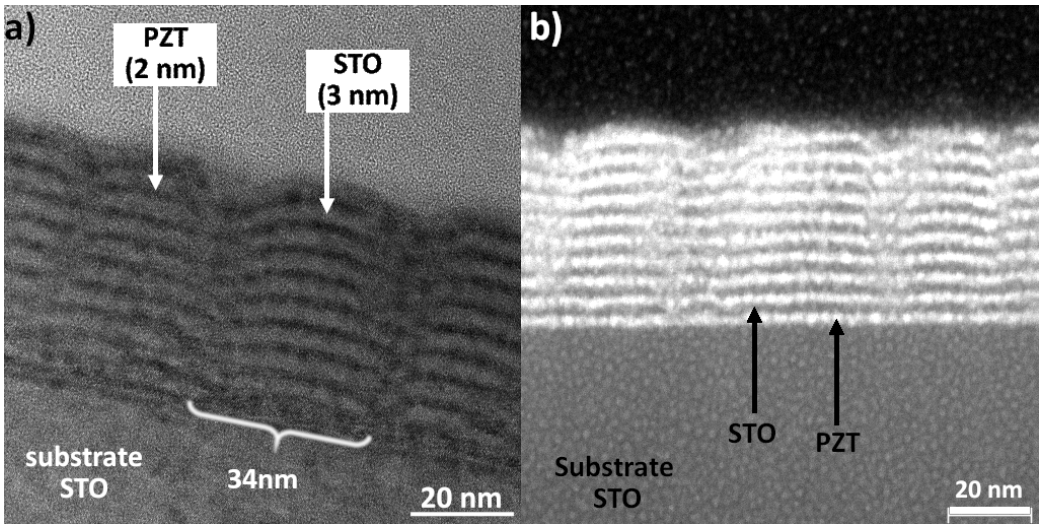

Fig. 2. (a) TEM micrograph of the PZT/STO SL in which the darker (greyer) layers correspond to PZT (STO) and b) associated STEM-HAADF image which is of opposite contrast to the TEM image.

Indirect additional evidence for the existence of a polar nanodomain structure in the sample is our determination of the Curie temperature. In Fig 3 we plot the average c-axis lattice parameter as a function of temperature. A decrease of this parameter, due to the

129 reduction of the out-of-plane component of polarization on approaching the
130 cubic/tetragonal phase transition, is observed. The Curie temperature is around 375 °C
131 and thus significantly lower than the reported value of 460°C for bulk PZT. This result is
132 not common in epitaxially grown thin films since strain is reported to push the transition
133 to higher temperature than in bulk. However bulk-like or even lower Tc values have been
134 reported in c- axis oriented thin films [2],[14] and more recently in
135 ferroelectric/paraelectric PT-based SLs [15],[16] despite epitaxial strain effects. Their
136 common feature is a destabilization of the ferroelectricity by the depolarizing field and
137 the resulting occurrence of 180° domains, at the origin of a lowering Tc which has also
138 been justified theoretically [17]. This feature is coherent with the detection of
139 nanodomains by XRD.
140
141

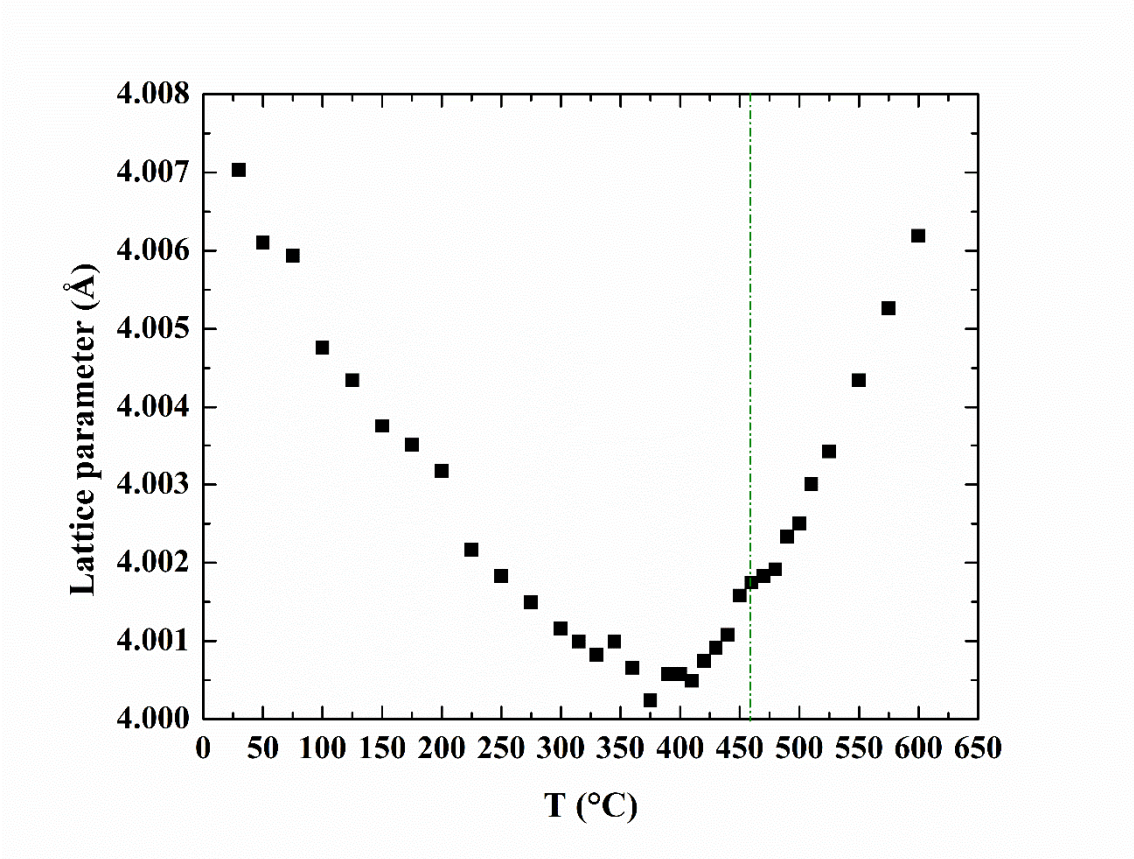

142

Fig. 3. Temperature dependence of the average out-of-plane c axis lattice parameter for the ($[PZT_5/STO_6]_{10}$) SL. The dotted line marks the Curie temperature of bulk PZT.

4. Conclusion

The ferroelectric/paraelectric SLs constitute flexible model systems to investigate the effects of strain and electrostatics on ferroelectric nanostructures like 180° domain structure. XRD is commonly used to evidence 180° stripe domains through the detection of satellite peaks characteristics of the ferroelectric stripe period. Our XRD and TEM investigations performed on a PZT/STO SL, clearly show that in such samples characterized by a noticeable misfit strain, the detection of diffuse scattering peaks can originate either from ferroelectric 180° nanodomains or from modulation related to elastic relaxation. It is shown that TEM investigations are required to disentangle elastic relaxation and ferroelectric domain contributions to in plane scattering profiles.

Acknowledgements

This work was supported by the region of Hauts de France and the European Fund for Economic and Regional Development FEDER. We thank Prof. M. G. Karkut for useful discussions.

References

[1] J. Íñiguez, P. Zubko, I. Luk'yanchuk, A. Cano, Nat. Rev. Mater. (2019).

[2] S.K. Streiffer, J.A. Eastman, D.D. Fong, C. Thompson, A. Munkholm, M.V. Ramana Murty, O. Auciello, G.R. Bai, G.B. Stephenson, Thin Films, Phys. Rev. Lett. 89 (2002) 067601.

169 [3] R. Takahashi, O. Dahl, E. Eberg, J.K. Grepstad, T. Tybell, J. Appl. Phys. 104 (2008)
170 064109.
171 [4] P. Zubko, N. Jecklin, N. Stucki, C. Lichtensteiger, G. Rispens, J.-M. Triscone,
172 Ferroelectrics. 433 (2012) 127–137.
173 [5] N. Lemée, I.C. Infante, C. Hubault, A. Boulle, N. Blanc, N. Boudet, V. Demange,
174 M.G. Karkut, ACS Appl. Mater. Interfaces. 7 (2015) 19906–19913.
175 [6] A.K. Yadav, C.T. Nelson, S.L. Hsu, Z. Hong, J.D. Clarkson, C.M. Schlepütz, A.R.
176 Damodaran, P. Shafer, E. Arenholz, L.R. Dedon, D. Chen, A. Vishwanath, A.M.
177 Minor, L.Q. Chen, J.F. Scott, L.W. Martin, R. Ramesh, Nature. 530 (2016) 198–
178 201.
179 [7] V.M. Kaganer, O. Brandt, A. Trampert, K.H. Ploog, Phys. Rev. B. 72 (2005).
180 [8] A.H.G. Vlooswijk, B. Noheda, G. Catalan, A. Janssens, B. Barcones, G. Rijnders,
181 D.H.A. Blank, S. Venkatesan, B. Kooi, J.T.M. de Hosson, Appl. Phys. Lett. 91
182 (2007) 112901.
183 [9] C. Hubault, C. Davoisne, A. Boulle, L. Dupont, V. Demange, A. Perrin, B. Gautier,
184 J. Holc, M. Kosec, M.G. Karkut, N. Lemée, J. Appl. Phys. 112 (2012) 114102.
185 [10] A. Boulle, I.C. Infante, N. Lemée, J. Appl. Crystallogr. 49 (2016) 845–855.
186 [11] P. Zubko, N. Jecklin, A. Torres-Pardo, P. Aguado-Puente, A. Gloter, C.
187 Lichtensteiger, J. Junquera, O. Stéphan, J.-M. Triscone, Nano Lett. (2012).
188 [12] L.E. Shilkrot, D.J. Srolovitz, J. Tersoff, , Appl. Phys. Lett. 77 (2000) 304.
189 [13] C. Hubault, C. Davoisne, L. Dupont, A. Perrin, A. Boulle, J. Holc, M. Kosec, M.G.
190 Karkut, N. Lemée, Appl. Phys. Lett. 99 (2011) 052905.
191 [14] D.D. Fong, G.B. Stephenson, S.K. Streiffer, J.A. Eastman, O. Auciello, P.H. Fuoss,
192 C. Thompson, Science. 304 (2004) 1650–1653.
193 [15] P. Zubko, N. Stucki, C. Lichtensteiger, J.-M. Triscone, Phys. Rev. Lett. 104 (2010)
194 187601.

195 [16] P. Zubko, N. Jecklin, N. Stucki, C. Lichtensteiger, G. Rispens, J.-M. Triscone,
196 Ferroelectrics. 433 (2012) 127–137.
197 [17] G.B. Stephenson, K.R. Elder, J. Appl. Phys. 100 (2006) 051601-051601-17.
198